

Effect of Sn additions on the age hardening response, microstructures and corrosion resistance of Mg-0.8Ca (wt%) alloys

C.L. Mendis, D. Tolnai, C. Blawert and N. Hort

MagIC -Magnesium Innovation Centre, Helmholtz Zentrum Geesthacht,
Institute for Materials, Max Planck Strasse 1 Geesthacht 21502, Germany

Keywords: Mg-Ca-Sn alloys, Microstructures, Age hardening

Abstract

The as-cast Mg-3Sn-2Ca alloy shows a good creep resistance that is better than that of AE42 alloy. The high content of alloying additions in these alloys results in low ductility due to the presence of primary intermetallic particles. The effect of reduced amount of Ca and Sn, below the maximum solid-solubility limit of each alloy additive, was studied to determine the potential of the Mg-0.8Ca-xSn alloys in structural applications. The microstructure of the alloys resulting from different processing routes was characterized and the corrosion resistance of the alloys measured to determine the best combination of alloy composition for further alloy development.

Introduction

Magnesium alloys have been considered in many applications where a combination of light weight and high specific strength is of importance. However, there is a lack of low cost, high strength magnesium alloys that may be used in structural applications where elevated temperature stability is required for temperatures up to 200°C. Mg-3Sn-2Ca (wt%) alloy has been recently developed as a possible high strength creep resistant alloy that has comparable creep resistance to AE42 alloys [1,2]. However the ductility to failure and the corrosion resistance of Mg-3Sn-2Ca alloy is not sufficient for many applications [2]. The high content of alloying additions found in this alloy cause formation of high volume fraction of primary intermetallic particles, which result in low ductility and corrosion resistance observed in the previous investigations [1,2]. The reduction in the volume fraction of intermetallic particles found in the alloys is expected to enhance the corrosion resistance but at a cost of reducing tensile yield strength. For improved ductility and corrosion resistance a magnesium alloy that contains lower content of alloying additions is very attractive. Precipitation hardening does not significantly reduce the ductility of heat treated, extruded or hot rolled magnesium alloys significantly [3]. This concept may be used to enhance the strength of magnesium alloys without significant loss in yield strength while retaining ductility of the alloy due to lower total solute concentration. The precipitation hardened Mg-Ca-Zn alloys with low solute contents has been shown to have a good combination of yield strength and ductility by Gao *et al.* [4] compared to a heat treated AZ91 alloy while the creep resistance of the alloy is relatively high. It is noted that the grain boundaries of the alloys investigated do not contain intermetallic particles that provide galvanic sites, which promote corrosion in many alloys strengthened by grain boundary intermetallic particles. It has been also shown for die cast AXJ530 alloy the creep resistance may be enhanced with precipitation of fine scale particles following the T6 heat treatment at 250°C [5].

Recently, a number of publications have shown that the ternary additions of Al [6], Zn [7-9] and In [10] have enhanced the age hardening response at 200°C for Mg-0.5Ca alloy (wt%). Each of these alloys was strengthened via a high density of very fine scale precipitates distributed uniformly through the microstructure. These precipitates are only few atomic layers in thickness and form on the basal planes for the Mg-Ca-Al [6] and Mg-Ca-Zn [9] alloys but form on the prismatic planes for the Mg-Ca-In alloys [6,10]. The refinement of precipitate distribution has been attributed to the negative enthalpies of mixing between the two alloying additions which has been proposed to enhance the nucleation of precipitates as compared with the binary alloy [11]. The enthalpy of mixing between Sn and Ca in the binary Sn-Ca system is reported to be negative [12] and thus expected the fine distribution of precipitates in the Mg-Ca-Sn alloys to enhance the precipitation hardening response of the alloy as compared with the binary Mg-Ca alloy.

In this paper we report the findings from a preliminary investigation on the as-cast and heat treated microstructures of Mg-0.8Ca-xSn (wt%) alloys with varying additions of Sn. The age hardening response of the Mg-0.8Ca-xSn (wt%) alloys was also evaluated at 200°C.

Experimental procedure

Pure Mg (99.99% Hydro Magnesium), was melted in a mild steel crucible and pure Sn (99.995% Chempur) and pure Ca (99% Alfa Aersar) was added to the melt at 700°C. The melt was held at ~700°C for 5 min stirred and then cast into a hardened steel finger mould pre-heated to 250°C. The nominal compositions of the alloys prepared are reported in Table 1. The samples of Mg-0.8Ca-xSn (wt%) was solution heat treated at 525°C for 5h in flowing Ar + SF₆ to prevent oxidation of the alloys. The samples were then cold water quenched to ensure dissolution of alloying additions. The samples for age hardening experiments were heat treated at 200°C for various times immediately following the solution heat treatment to ensure maximum amount of solute is available for precipitation. The age hardening response was measured after different ageing times at 200°C by measuring the Vickers hardness on samples ground to a 2500 grit SiC paper finish using an EMCOTEST MIC10 Vickers hardness tester with a load of 5kg. The hardness values reported are an average of 10 measurements for each of the testing conditions.

The samples were ground with SiC paper to 2500 grit finish and then polished in 3µm diamond suspension and a mixture of 1µm diamond suspension and OPS suspension for optical microscopy and scanning electron microscopy (SEM). SEM investigations were conducted with a Carl Zeiss ULTRATM 55 SEM equipped with an EDAX energy dispersive X-ray spectrometer.

The intermetallic phases found in the as-cast and the solution heat treated samples were characterized at the BW2 beam line of the Hamburger Synchrotronstrahlungslabor (HASYLAB) at the Deutsches Elektronen-Synchrotron (DESY). The high brilliance of the beam allows the detection of the low volume fraction intermetallic phases. The beam energy was set to 100 keV. During the experiment the diffraction patterns were recorded with a 10s acquisition time by a mar555 flatpanel with an area of 3070×2560 pixels with a pixel size of 140 μm².

Table 1 Nominal compositions of the alloys investigated

Alloy	Composition (wt%)		
	Mg	Ca	Sn
Mg-0.8Ca-	balance	0.8	-
Mg-0.8Ca-1.2Sn	balance	0.8	1.2
Mg-0.8Ca-2.3Sn	balance	0.8	2.3
Mg-0.8Ca-3.5Sn	balance	0.8	3.5

Preliminary analyses of precipitate microstructures were conducted in a Phillips CM200 transmission electron microscope operating at 200 kV. The samples for TEM analysis were prepared by electric discharge machining 3 mm discs from alloy specimens that were ~ 200 mm in thickness and twin jet electropolishing using a solution of 1.5% perchloric acid in methanol at a polishing temperature of ~-45°C with a current of ~0.8-1.2mA and a voltage of 50V. Upon perforation the specimens were washed in ethanol to remove any trace of acid.

Potential-dynamic polarization tests for the as-cast Mg-0.8Ca-xSn alloys were conducted in 0.5%NaCl solution with starting pH of 7. Measurements were conducted with standard 3 electrode cell (330ml) method where the sample was the working electrode

while the counter electrode was platinum mesh. The reference electrode used in this experiment was Ag/AgCl. The free corrosion potential was measured after 30mins and the polarization curve was measured at a scan rate of 0.2mVs⁻¹ and the corrosion rate was determined from the corrosion current at the intersection of the cathodic Tafel slope with the vertical through the corrosion potential.

Results and discussion

The as-cast and the solution heat treated microstructures

The optical micrographs of the as-cast and the solution treated Mg-0.8Ca-xSn alloys are shown in Figure 1. The as-cast microstructures, Fig 1 (a-c) show the presence of a semi continuous to continuous network of primary intermetallic particles at the grain boundaries and in the inter-dendritic regions. The solution treated samples of Mg-0.8Ca-xSn alloys, Fig 1 (d-f) showed a significant reduction in the volume fraction of intermetallic particles found at the grain boundaries. Additionally, solution heat treatment removed the dendritic nature of the microstructure and caused some grain growth in the alloys investigated. The change in the microstructure from the as-cast samples to the solution heat treated samples may be clearly observed in SEM microstructures shown in Fig 2. The microstructures of Mg-0.8Ca-3.5Sn alloy is shown here as an example which shows the changes to contrast along the dendrites showing changes in the composition of the alloy, Fig 2 (a), in the as-cast condition which is not evident in the solution heat treated alloy of the same composition, Fig. 2(b).

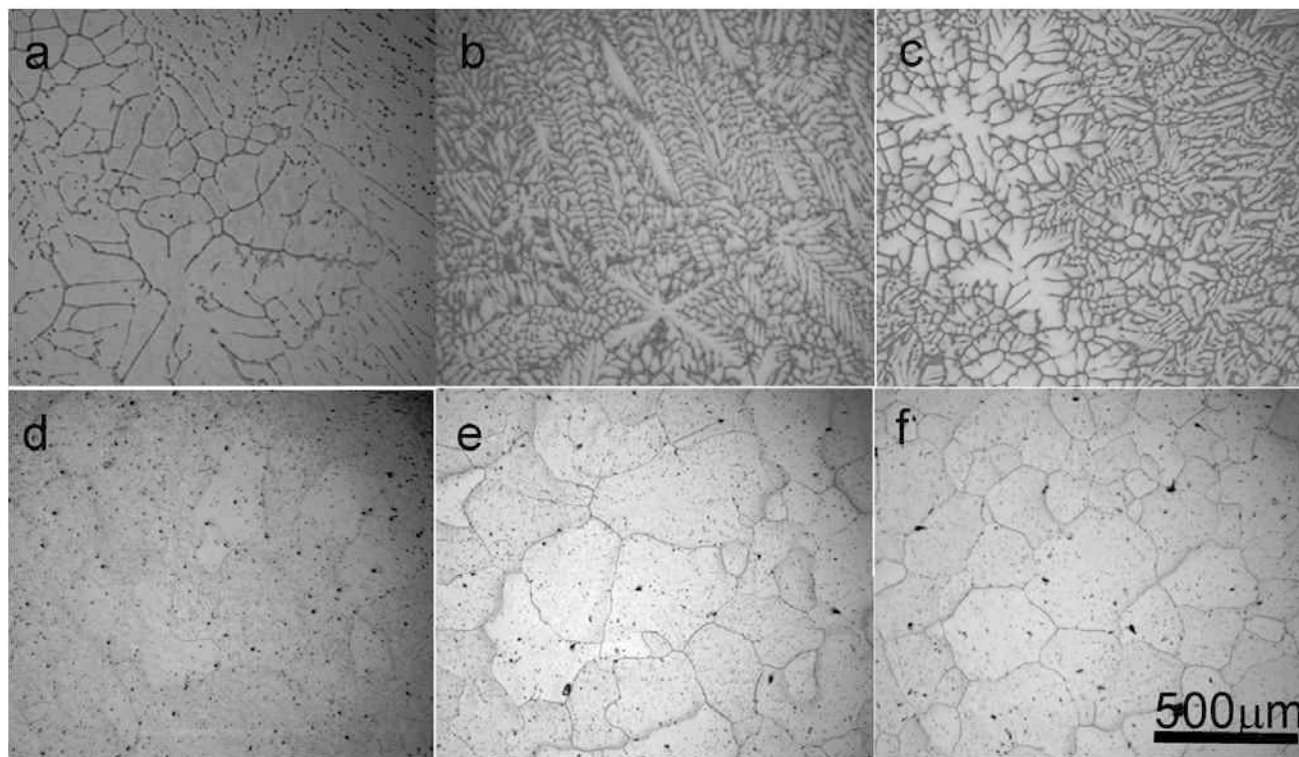


Figure 1. Optical micrographs typical of (a-c) the as-cast and (d-f) the solution heat treated 525°C/5h alloys. (a,d) Mg-0.8Ca-1.2Sn (b,e) Mg-0.8Ca-2.3Sn and (c,f) Mg-0.8Ca-3.5Sn

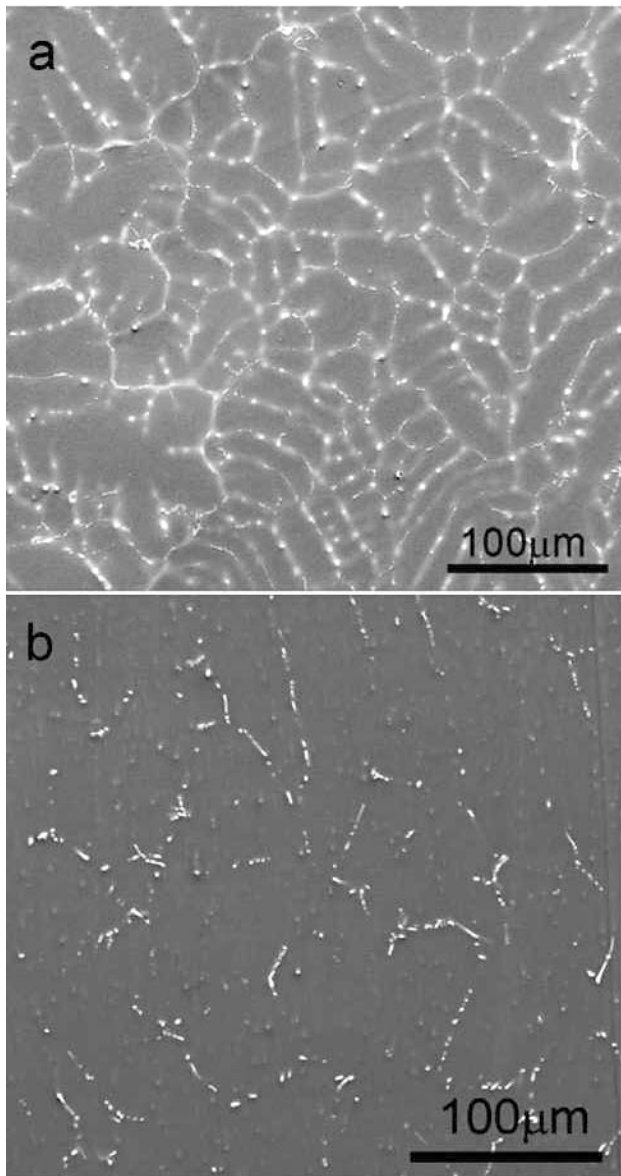


Figure 2 SEM micrographs showing (a) the as-cast and (b) the solution heat treated at 525°C/5h microstructures of Mg-0.8Ca-3.6Sn alloy.

Two dimensional diffraction patterns were recorded during synchrotron diffraction measurements. The Debye-Scherrer rings were integrated through 360° to obtain the line profiles shown in Fig 3. These line profiles show that in the as-cast samples, Fig 3 (a) the main peaks are due to magnesium while some additional peaks due to intermetallic phases could also be observed. In the Mg-0.8Ca alloy some very small reflections due to Mg₂Ca may be observed but the main peaks due to Mg₂Ca phase are overlapping with the magnesium peaks in the line profile. In Mg-0.8Ca-xSn alloys the MgSnCa phase (orthorhombic crystal structure with $a = 0.786\text{nm}$ $b = 4.66\text{nm}$ $c = 8.74\text{nm}$ [13]) was observed in addition to the peaks due to magnesium. After the solution heat treatment, the peaks due to the intermetallic phases have largely disappeared from the line profiles and only peaks due to the magnesium may be observed, Fig 3 (b). It is noted that the magnesium peaks had shifted slightly from the position for the as-cast alloy of the same

composition. The shift in the peaks may be associated with the incorporation of solute elements into the matrix during solution heat treatment.

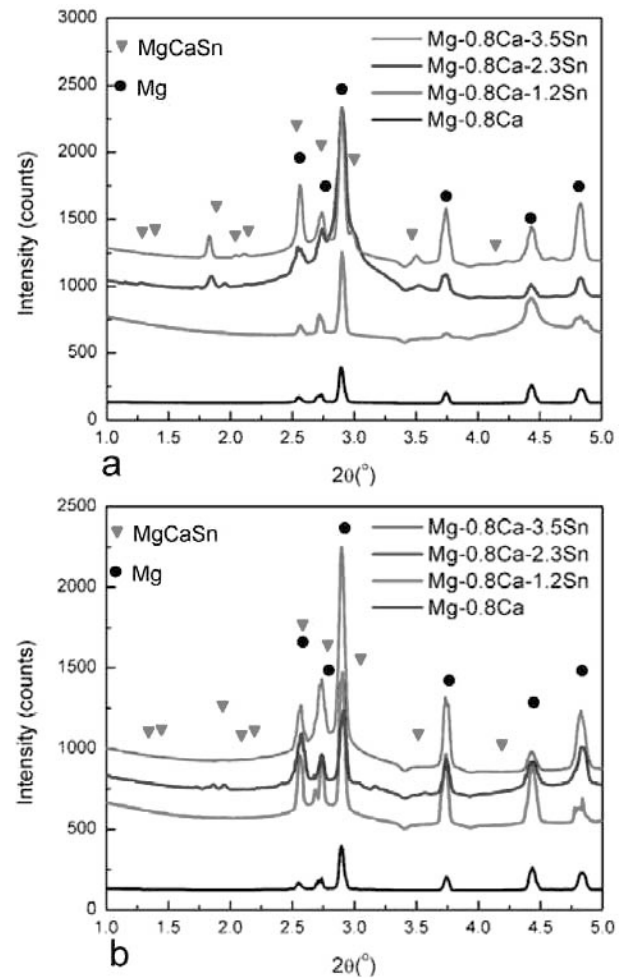


Figure 3 XRD line profiles resulting from the azimuthal integration of the diffraction patterns recorded from Mg-0.8Ca-xSn and Mg-0.8Ca alloys in (a) the as-cast and (b) solution heat treated 525°C/5h conditions (Wavelength $\lambda = 0.0124\text{ nm}$)

Corrosion resistance of the as-cast microstructures

The pertinent results from the potentiodynamic polarization curves are listed in Table 2. The free corrosion potential and the I_{corr} measured increases with increased Sn concentration. It is obvious that the nobler Sn and Sn-based intermetallics are responsible for the observed increase in the free corrosion potential. Furthermore the intermetallics can cause internal galvanic corrosion thus the increase in the corrosion rate is consistent with the increase in the volume fraction of the intermetallic phases. The Mg-0.8Ca-1.2Sn alloy shows with a 1.1mm/year the lowest rate of corrosion and the Mg-0.8Ca-3.5Sn with a 1.5mm/year the highest. The corrosion curves, not shown in this contribution, show that passivation of the corroded samples was observed. This is especially evident in the Mg-0.8Ca-1.2Sn alloy. This suggests that the Mg-0.8Ca-xSn alloys show good potential as a structural magnesium alloy.

Table 2 Pertinent features from the potentiodynamic corrosion curves of the as-cast Mg-0.8Ca-xSn alloys.

	Alloy		
	Mg-0.8Ca-1.2Sn	Mg-0.8Ca-2.3Sn	Mg-0.8Ca-3.5Sn
E_{corr} (mV)	1756	1669	1651
I_{corr} (mA)	0.0477	0.0592	0.0683
Corrosion rate mm/y	1.09	1.39	1.47

Age hardening response and precipitate microstructures

The age hardening response of the Mg-0.8Ca-xSn alloys at 200°C are shown in Fig 4 (a). The age hardening response of the Mg-0.8Ca alloy is relatively small and a hardness increment of only 9VH was observed. The addition of Sn to the Mg-0.8Ca resulted in an increase in the maximum hardness observed by two times while it also decrease the time to peak hardness from ~16h in the binary alloy to ~10h in the ternary alloys. The maximum hardness increment was observed for the Mg-0.8Ca-3.5Sn alloy after ageing for 10h. The TEM micrographs illustrating the precipitate microstructure of the peak aged Mg-0.8Ca-3.5Sn alloy is shown in Fig. 4 (b). The conventional TEM micrographs show that the precipitate particles form on the basal planes of magnesium with a particle diameter of $\sim 20 \pm 5$ nm, but the particle thickness cannot be measured accurately from conventional TEM images. The diffraction pattern recorded $\langle 10\bar{1}0 \rangle_{\text{Mg}}$, Fig 4 (b insert), show additional diffraction contrast due to solid-state precipitates. The diffused line like contrast associated with the precipitates suggests that these particles are very thin in the thickness direction as compared with the diameter of the precipitates. The diffraction contrast due to the precipitate particles in Mg-0.8Ca-Sn alloy is similar to that observed for the Mg-0.5Ca-1.2Zn [7-9] and Mg-0.5Ca-0.5Al [6] alloys in previous investigations. The diffraction patterns and precipitate morphology suggest that the precipitates observed in the Mg-0.8Ca-Sn are of the same morphology as the previous investigations.

Conclusions

The Sn addition to Mg-0.8Ca alloy resulted in the formation of MgCaSn phase at the grain boundaries in the as-cast condition which was dissolved into the magnesium matrix by solution heat treatment in all alloys with the exception of the Mg-0.8Ca-3.5Sn alloy.

A relatively low corrosion rate was observed for the Mg-0.8Ca-xSn alloys in the as-cast condition with the Mg-0.8Ca-1.2Sn alloy showing the lowest corrosion rate, thus the best resistance to corrosion.

The age hardening experiments at 200°C showed that the hardness of Mg-0.8Ca-xSn alloys increased with the addition of Sn compared to the binary Mg-0.8Ca alloy. The maximum hardening response was from the Mg-0.8Ca-3.5Sn alloy.

The hardening increment was due to a uniform distribution of very thin basal plate precipitates forming in the peak-aged alloy thought to be similar to those observed in Mg-Ca-Zn and Mg-Ca-Al alloys previously under heat treatment conditions.

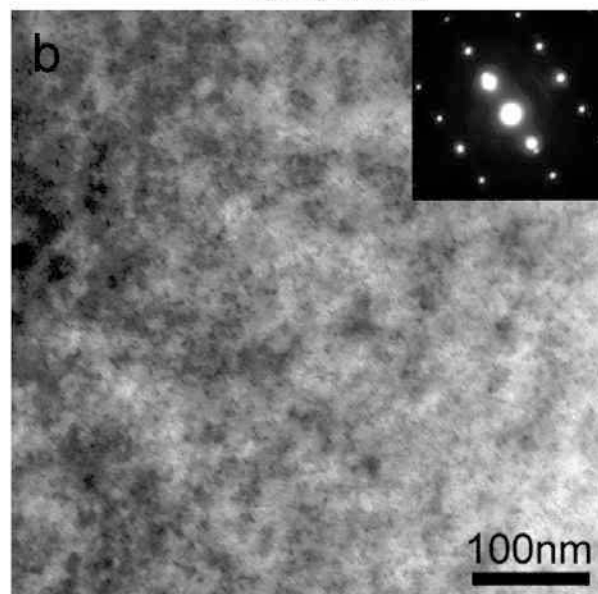
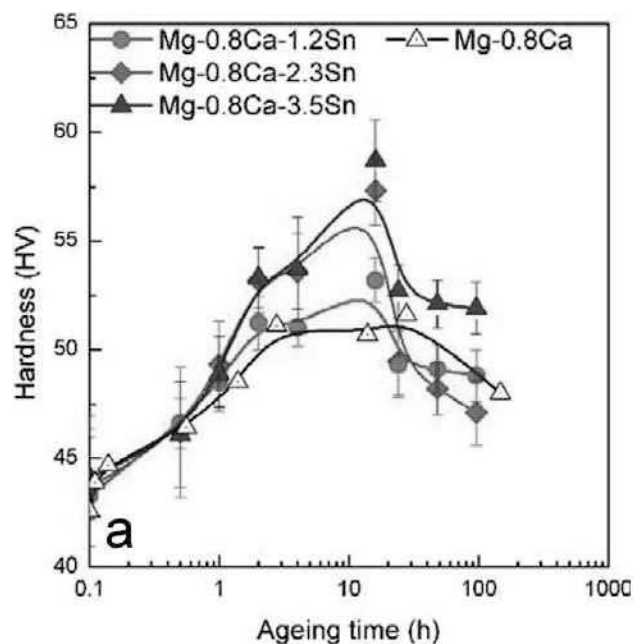


Figure 4 (a) the age hardening response of Mg-0.8Ca-xSn alloys at 200°C. (b) The precipitate microstructure of Mg-0.8Ca-3.5Sn alloy aged at 200°C for 10h to peak hardness. Electron beam is approximately parallel to $\langle 10\bar{1}0 \rangle_{\text{Mg}}$.

Acknowledgements

The authors would like to thank the Deutsches Elektronen-Synchrotron the provision of synchrotron radiation facilities in the framework of the proposal II-20100225.

References

1. N. Hort *et al*. Microstructural Investigations of the Mg-Sn-xCa system *Advanced Eng. Mater* 8 (2006) 359-364
2. T.Abu Leil *et al* Microstructure corrosion and creep of as-cast magnesium alloys In *Magnesium Technology 2007* (Ed R. Beals M.O. Pekguleryux R. Neelameggham and A.A. Luo) TMS Materials Park Ohio (2007)
3. K. Hono *et al* Towards the development of heat-treatable high-strength wrought Mg alloys *Scripta Mater.* 63 (2010) 710-15.
4. X. Gao *et al* Precipitation-hardened Mg–Ca–Zn alloys with superior creep resistance *Scripta Mater* 53 (2005) 1321-26.
5. A. Suzuki *et al* Precipitation strengthening of a Mg-Al-Ca-Based AXJ530Die-cast Alloy *Metall. Mater. Trans. A.* 39A (2008) 696-702.
6. J. Jayamani *et al* Enhanced precipitation hardening of Mg-Ca alloy by Al additions *Scripta Mater* 63 (2010) 831-34
7. J.F. Nie and B.C. Muddle Precipitation hardening of Mg-Ca-(Zn) alloys 37 (1997) 1475-81
8. J.C. Oh *et al* TEM and 3DAP characterization of an age-hardened Mg–Ca–Zn alloy *Scripta Mater* 53 (2005)675-679
9. K. Oh-ishi *et al* Age hardening response of Mg-0.3at.%Ca alloys with different Zn contents *Mater Sci Eng A* 526 (2009)177-84
10. C.L. Mendis *et al* Precipitation of prismatic plates in Mg-0.3Ca alloys with In additions *Scripta Mater.* 64 (2011) 137-40
11. C.L. Mendis *et al* Microalloying effect on the precipitation processes of Mg-Ca alloys *Metall. Mater Trans A* 43 (2012) 3978-87
12. F. R. de Boer *et al* Cohesion in Metals : Transition Metal alloys (Cohesion and Structure) (1989) Elsevier New York
13. Villars, P. and Calvert, L.D., Pearson's Handbook of Crystallographic Data for Intermetallic Phases. 2nd ed (1991) ASM International, Materials Park Ohio.